Signal Processing 94 (2014) 359–372

Contents lists available at ScienceDirect

Signal Processing

journal homepage: www.elsevier.com/locate/sigpro

Fractional Hilbert transform extensions and associated analytic signal construction

Arun Venkitaraman, Chandra Sekhar Seelamantula *

Department of Electrical Engineering, Indian Institute of Science, Bangalore 560012, India

ARTICLE INFO

Article history:
Received 17 November 2012
Received in revised form
10 March 2013
Accepted 8 May 2013
Available online 22 May 2013

Keywords:
Hilbert transform
Fractional Hilbert transform
Analytic signal
Single-sideband modulation
Generalized-phase Hilbert transform
Generalized-phase analytic signal

ABSTRACT

The analytic signal (AS) was proposed by Gabor as a complex signal corresponding to a given real signal. The AS has a one-sided spectrum and gives rise to meaningful spectral averages. The Hilbert transform (HT) is a key component in Gabor's AS construction. We generalize the construction methodology by employing the fractional Hilbert transform (FrHT), without going through the standard fractional Fourier transform (FrFT) route. We discuss some properties of the fractional Hilbert operator and show how decomposition of the operator in terms of the identity and the standard Hilbert operators enables the construction of a family of analytic signals. We show that these analytic signals also satisfy Bedrosian-type properties and that their time–frequency localization properties are unaltered. We also propose a generalized-phase AS (GPAS) using a generalized-phase Hilbert transform (GPHT). We show that the GPHT shares many properties of the FrHT, in particular, selective highlighting of singularities, and a connection with Lie groups. We also investigate the duality between analyticity and causality concepts to arrive at a representation of causal signals in terms of the FrHT and GPHT. On the application front, we develop a secure multi-key single-sideband (SSB) modulation scheme and analyze its performance in noise and sensitivity to security key perturbations.

1. Introduction

The analytic signal formalism proposed by Gabor [1] is a methodology for constructing a unique complex signal associated with a given real signal. The complex signal is derived by adding the real signal in quadrature with its Hilbert transform. As a consequence of this construction, the spectrum vanishes for negative frequencies. The amplitude-modulation (AM) and phase-modulation (PM) of an AM–frequency-modulated (AM–FM) signal are defined as the modulus and phase of the AS, respectively [2–5]. The AS allows for meaningful computations of the mean frequency and bandwidth, which are crucial in computing the time-bandwidth product and in determining the time–frequency localization properties governed by Heisenberg's uncertainty principle. The analytic nature of the signal can be retained while allowing for specific properties on the AM, FM, or PM. For example, to have a nonnegative FM, finite Blaschke products (which are essentially time-domain duals of allpass filters that signal processing community is more familiar with) have been considered by Picinbono [6], Kumaresan–Rao [7], and Doroslovački [8], which were further extended to an infinite product by Dang and Qian [9], who provided a systematic study of minimum-phase and allpass factorization of analytic signals. Specific results in the context of analytic representations with bandlimited AM have been derived by Xia et al. [10] and Deng and Qian [11]. Another class of generalizations concerning the analytic signal representation are given in terms of employing FrFT, which are reviewed in Section 1.1.

In this paper, we develop a generalization of Gabor's construction using the FrHT without using the FrFT. We

* Corresponding author. Tel.: +91 80 22932695; fax: +91 80 23600444.
E-mail addresses: arun.venkitaraman@gmail.com (A. Venkitaraman), chandra.sekhar@ieee.org (C.S. Seelamantula).

0165-1684/$ - see front matter © 2013 Elsevier B.V. All rights reserved.
http://dx.doi.org/10.1016/j.sigpro.2013.05.009

also propose another generalization of our method, which relies on a functional extension of the HT.

1.1. Review of related work

One of the early works in connection with FrHTs is that of Lohmann et al. [12], who proposed two fractional generalizations of the classical HT. They proposed optical implementations of the FrHT using spatial filtering. One of the generalizations is based on a modification of the spatial filter using a fractional parameter, and the other one is based on the FrFT [13,14]. They also provided a unified definition resulting from a combination of the spatial filter and FrFT approaches. Davis et al. [15] employed the FrHT of Lohmann et al. for edge detection and showed that as the fractional order is varied, one can obtain different qualities of edge enhancement and also achieve selective highlighting of rising or falling edges. Pei and Yeh [16] also deployed the FrHT for similar applications based on a discrete counterpart of the FrHT. Zayed [17] took the AS formalism associated with the standard Fourier transform (FT) and provided a counterpart of it for the FrFT. This procedure is anchored on the FrFT and requires a generalization of the HT, which is obtained by multiplying the time-domain function with a chirp, passing the product through the standard HT, and then dechirping the output to obtain the corresponding AS. Tseng and Pei [18] considered optimized design strategies for finite impulse response (FIR) designs and infinite impulse response (IIR) models of the discrete-time FrHT, and proposed a novel secure SSB communication application using the angle of the FrHT as a secure key. An interesting aspect of their design is that since the FrHT is an allpass filter, much like the HT, rational allpass filter forms are used to approximate the FrHT. Pei and Wang proposed the design of discrete FrHT using maximally flat FIR filters whose impulse responses were obtained in simple analytical form, and devised efficient hardware realizations for both odd and even order filters [19]. Cusmariu proposed three extensions of Gabor's AS using the FrHT, called fractional analytic signals, which reduce to Gabor's AS when the FrHT angle is set to $\pi/2$ [20]. The first fractional AS definition is based on a rotation of Gabor's AS, the second is obtained by using the FrHT as the imaginary part, and the third is obtained as a weighted linear combination of the signal and its standard HT. In particular, it was shown in this work that the FrHT has the semi-group property, unlike the GHT proposed by Zayed. However, fractional analytic signals do not always have a one-sided spectrum. Tao et al. [21] pursued a similar philosophy as that of Zayed and proposed an analytic counterpart associated with the FrFT in conjunction with the FrHT, using time-domain chirping, standard HT, and dechirping. The fundamental issue addressed by Tao et al. is that since the FrFT does not exhibit conjugate symmetry, suppressing the negative part of the frequency spectrum requires some care; otherwise, one may not be able to recover the real signal from the analytic counterpart [21]. On the application front, they proposed a SSB modulation scheme, which uses the angle of the FrFT and the phase of the FrHT as secret keys for demodulation. Fu and Li proposed a generalization of the AS through the linear canonical transform (LCT) domain [22]. Their formalism is based on the parameterized HT, which includes the FrFT-based HT [17] as a special case, and the LCT-based generalized AS is obtained by taking the inverse-LCT after suppressing its negative frequency spectrum. A generalized Bedrosian theorem associated with the LCT was also proposed by Fu and Li. Guanlei et al. [23] proposed different definitions of two-dimensional HT in the LCT domain and discussed different properties, with particular emphasis on the relation between the time-domain and transformed domain mappings. Sarkar et al. proposed a generalization of the HT based on the generalization of decay of the impulse response of the standard HT kernel and applied it for symbolic time series analysis of noise-corrupted dynamical systems [24]. They also proposed an AS counterpart using the generalized HT, which results in functions with one-sided spectra only for certain values of the decay parameter. An all-optical implementation of the FrHT using a phase-shifted fiber Bragg grating was proposed by Ge et al. [25], capable of operating on input waveforms with bandwidths up to hundreds of Gigahertz. Chaudhury et al. [26] deployed the FrHT in the representation of the dual-tree complex wavelet transforms based on the shifting action of the FrHT operator. They also introduced a generalization of the Bedrosian identity for the FrHT, and extended the concepts to the multidimensional setting by proposing a directional FrHT.

1.2. This paper

In this paper, we address the aspect of AS construction starting with the FrHT, but by employing the standard FT and without taking the FrFT route. In fact, it turns out that the properties of the spectra associated with FrHT operators and the approach presented in this paper do not necessitate the use of FrFT. We recall some properties of the FrHT vis-a-vis those of the HT. We show how our framework leads to the generation of a family of analytic signals, one corresponding to every value of the phase parameter of the FrHT. We show that the FrHT approach for AS construction enables a natural geometric interpretation. We carry out the analytical developments and construction of a generalization of the AS in the continuous-domain, which we refer to as the $\phi-$AS, for which we favor a Hilbert space formalism and work with suitably defined operators. We also seek to analyze some specific properties of the $\phi-$AS, namely, AM/FM separation, operator invariances, factorization properties, energy preservation, temporal and spectral moments, and the associated Heisenberg uncertainty principle. We also propose a new member to the family of Hilbert transforms, called the generalized-phase Hilbert transform (GPHT), which is based on a functional generalization of the FrHT phase. We show that the properties of the FrHT, in particular, the enhancement and selective highlighting of edges, are preserved in the process of generalization. A connection between Lie groups and the GPHT is also presented. The GPHT is then used to construct a generalized $\phi-$AS construction, called the generalized-phase analytic signal. We show that the GPAS is related to Gabor's AS by a linear filtering operation. By analyzing the link between causality and analyticity, we show how causal signals can be characterized using the FrHT/GPHT. As an application of the developed concepts, we propose a multi-key secure

SSB scheme and demonstrate its robustness to SSB-key perturbations and additive noise.

In Section 2, we propose a construction of ϕ−AS. We discuss some properties of the ϕ−AS in Section 3. The GPHT is proposed in Section 4. In Section 5, we propose an extension to the ϕ−AS using the GPHT. In Section 6, we show how causal signals can also be characterized using the FrHT/GPHT. In Section 7, we propose a secure SSB scheme using the GPHT proposed in Section 4.

1.3. Notations

The symbols $\langle\cdot,\cdot\rangle$ and $\|\cdot\|$ denote the $\mathbf{L}^2$ inner-product and norm, respectively. We use $\hat{f}(\omega)$ to denote the FT of the function $f(t)$, $\mathcal{F}$ to denote the Fourier operator, $\mathcal{H}$ for the Hilbert operator, and $\tilde{f}(t)$ to denote the HT of $f(t)$. Therefore, $\hat{f}(\omega)=\mathcal{F}\{f\}(\omega)$, and $\tilde{f}(t)=\mathcal{H}\{f\}(t)$. The symbol $\mathcal{H}_\phi$ denotes the fractional Hilbert operator, and $*$ denotes the convolution operator. We use $\mathcal{S}_\tau$ and $\mathcal{D}_\sigma$ to denote the shift and dilation operators, respectively: $\mathcal{S}_\tau\{f\}(t)=f(t-\tau)$, and $\mathcal{D}_\sigma\{f\}(t)=f(t/\sigma)$.

2. The ϕ−analytic signal

2.1. Gabor's analytic signal

Consider a real-valued function $f(t)$, and its HT defined by

$$\tilde{f}(t)=\mathcal{H}\{f\}(t)=\text{p.v.}\ \frac{1}{\pi}\int_{-\infty}^{+\infty}\frac{f(\tau)}{t-\tau}\,\mathrm{d}\tau=(h*f)(t),$$

where $h(t)=1/\pi t$ is the Hilbert convolutional kernel and p.v. denotes the Cauchy principal value integral. The adjoint operator of $\mathcal{H}$ is given by $\mathcal{H}^\dagger=-\mathcal{H}$. The FT of $h(t)$ is specified in a distributional sense as $\hat{h}(\omega)=-\mathrm{j}\ \mathrm{sign}(\omega)$, where $\mathrm{j}=\sqrt{-1}$ and $\mathrm{sign}(\cdot)$ denotes the signum function. In the Fourier domain, we have the expression: $\hat{\tilde{f}}(\omega)=\hat{h}(\omega)\hat{f}(\omega)=-\mathrm{j}\ \mathrm{sign}(\omega)\hat{f}(\omega)$. Let $f^a(t)$ denote the AS of $f(t)$ constructed by adding f in quadrature with $\tilde{f}$ as follows: $f^a(t)=f(t)+\mathrm{j}\tilde{f}(t)$. $f(t)$ can be obtained from $f^a(t)$ as $f(t)=\mathrm{Real}\{f^a(t)\}$. In the frequency domain, the AS has the equivalent representation:

$$\hat{f}^a(\omega)=(1+\mathrm{sign}(\omega))\hat{f}(\omega)=2\hat{f}(\omega)\mathcal{U}(\omega),\tag{1}$$

where $\mathcal{U}(\cdot)$ denotes the unit-step function. The AS operator denoted by $\mathcal{A}$ can be represented as

$$\mathcal{A}=\mathcal{I}+\mathrm{j}\mathcal{H},\tag{2}$$

where $\mathcal{I}$ denotes the identity operator. Using this notation, $f^a(t)=\mathcal{A}\{f\}(t)$. We observe from (1) that the AS has a one-sided spectrum.

2.2. Fractional Hilbert operator

The fractional Hilbert kernel $h_\phi(t)$ corresponding to the FrHT operator $\mathcal{H}_\phi$ is specified in the Fourier domain as follows:

$$\hat{h}_\phi(\omega)=e^{-\mathrm{j}\phi\ \mathrm{sign}(\omega)}=e^{-\mathrm{j}\phi}\mathcal{U}(\omega)+e^{\mathrm{j}\phi}\mathcal{U}(-\omega),\tag{3}$$

where $-\pi/2\le\phi\le\pi/2$. Correspondingly, the fractional Hilbert operator $\mathcal{H}_\phi$ can be expressed as a linear combination of the identity and standard Hilbert operators [12,15,26]:

$$\mathcal{H}_\phi=\cos\ \phi\mathcal{I}+\sin\ \phi\mathcal{H}.\tag{4}$$

For $\phi=\pi/2$, the fractional Hilbert operator coincides with the standard Hilbert operator: $\mathcal{H}_{\pi/2}=\mathcal{H}$. On the other hand, for $\phi=0$, $\mathcal{H}_\phi$ reduces to the identity operator. The adjoint operator is given by $\mathcal{H}_\phi^\dagger=\mathcal{H}_{-\phi}$, such that $\mathcal{H}_\phi^\dagger\mathcal{H}_\phi=\mathcal{H}_{-\phi}\mathcal{H}_\phi=\mathcal{I}$.

The fractional Hilbert transform of $f(t)$ is obtained as

$$\begin{aligned}\tilde{f}_\phi(t)=\mathcal{H}_\phi\{f\}(t)&=\cos\ \phi f(t)+\sin\ \phi\mathcal{H}\{f\}(t)\\&=\cos\ \phi f(t)+\text{p. v.}\int_{-\infty}^{+\infty}\frac{\sin\ \phi}{\pi(t-\tau)}f(\tau)\,\mathrm{d}\tau=(h_\phi*f)(t),\end{aligned}$$

where $h_\phi(t)=\mathcal{F}^{-1}\{\hat{h}_\phi(\omega)\}=\cos\ \phi\delta(t)+\sin\ \phi 1/\pi t$ is the fractional Hilbert kernel.

2.3. Properties of the fractional Hilbert operator

(P1) *Linearity*: $\mathcal{H}_\phi\{\alpha_1 f_1+\alpha_2 f_2\}(t)=\alpha_1\mathcal{H}_\phi\{f_1\}(t)+\alpha_2\mathcal{H}_\phi\{f_2\}(t)$, for α_1 and α_2 in the complex field $\mathbb{C}$.
(P2) *Shift-invariance*: $\mathcal{S}_\tau\mathcal{H}_\phi\{f\}(t)=\mathcal{H}_\phi\mathcal{S}_\tau\{f\}(t)$, for $\tau\in\mathbb{R}$.
(P3) *Scale-invariance*: $\mathcal{D}_\sigma\mathcal{H}_\phi\{f\}(t)=\mathcal{H}_\phi\mathcal{D}_\sigma\{f\}(t)$, for $\sigma\in\mathbb{R}^+$.
(P4) *Orthogonality*: If $f,g\in\mathbf{L}^2(\mathbb{R})$ such that $f\perp g$, that is, $\langle f,g\rangle=0$, then $\langle\tilde{f}_\phi,\tilde{g}_\phi\rangle=0$.
(P5) *Linear independence*: If $\{f_i(t)\}_{i=1}^N$ constitutes a set of linearly independent functions, so does $\{\mathcal{H}_\phi\{f_i\}(t)\}_{i=1}^N$.

Properties (P1), (P2), and (P3) follow from the linearity, shift-invariance, and scale-invariance, respectively, of $\mathcal{H}$ and $\mathcal{H}_\phi$. The property (P4) may be proved by considering the inner product of $\tilde{f}_\phi$ and $\tilde{g}_\phi$:

$$\langle\tilde{f}_\phi,\tilde{g}_\phi\rangle=\langle\mathcal{H}_\phi\{f\},\mathcal{H}_\phi\{g\}\rangle=\langle f,\mathcal{H}_\phi^\dagger\mathcal{H}_\phi\{g\}\rangle=\langle f,g\rangle=0.$$

The proof of (P5) follows directly from the definition of linear independence and the linearity of $\mathcal{H}_\phi$. The property (P5) enables one to generate a new set of bases starting from a given set of linearly independent functions, and in particular has been applied to the construction of wavelet bases [26,27].

2.4. Construction of the ϕ−analytic signal

Let us construct a complex signal operator $\mathcal{A}_\phi$ such that

$$\mathcal{A}_\phi=\mathcal{I}+e^{\mathrm{j}(\pi-\phi)}\mathcal{H}_\phi,\tag{5}$$

and let $f_\phi^a(t)=\mathcal{A}_\phi\{f\}(t)=f(t)+e^{\mathrm{j}(\pi-\phi)}\mathcal{H}_\phi\{f\}(t)$. In the frequency domain, we get that

$$\begin{aligned}\hat{f}_\phi^a(\omega)&=\hat{f}(\omega)+e^{\mathrm{j}(\pi-\phi)}\hat{\tilde{f}}_\phi(\omega)=\hat{f}(\omega)+e^{\mathrm{j}(\pi-\phi)}\hat{h}_\phi(\omega)\hat{f}(\omega)\\&=(1-e^{-2\mathrm{j}\phi})\hat{f}(\omega)\mathcal{U}(\omega)=2\ \sin\ \phi e^{\mathrm{j}(\pi/2-\phi)}\hat{f}(\omega)\mathcal{U}(\omega),\end{aligned}\tag{6}$$

which vanishes for $\omega<0$. Therefore, $f_\phi^a(t)$ is analytic. Taking the inverse FT of $\hat{f}_\phi^a(\omega)$ gives

$$\begin{aligned}f_\phi^a(t)&=2\ \sin\ \phi e^{\mathrm{j}(\pi/2-\phi)}\frac{1}{2\pi}\int_0^\infty\hat{f}(\omega)e^{\mathrm{j}\omega t}\,\mathrm{d}\omega\\&=\sin\ \phi e^{\mathrm{j}(\pi/2-\phi)}f^a(t).\end{aligned}\tag{7}$$

We observe that Gabor's AS $f^a(t)$, and the generalized AS $f^a_\phi(t)$, are related by a complex scaling constant that depends on the FrHT parameter ϕ. Thus, $f^a_\phi(t)$ represents a family of analytic signals characterized by the parameter ϕ. We shall refer to $f^a_\phi(t)$ as the *$\phi-$analytic signal* ($\phi-AS$). Using (7), $f(t)$ is obtained from $f^a_\phi(t)$ as $f(t)=\operatorname{cosec}\phi\, e^{-\mathrm{j}(\pi/2-\phi)}\mathrm{Real}\{f^a_\phi(t)\}$. In Fig. 1(a) and (b), we provide a comparison of the construction of Gabor's AS and the $\phi-$AS, respectively.

2.5. Geometric interpretation of the $\phi-$AS construction

We next provide a geometric interpretation of the AS construction by treating functions as vectors. Using FTs, it can be shown that a function and its HT are orthogonal, that is, $\langle f,\tilde{f}\rangle=0$. The AS $f^a(t)=f(t)+\mathrm{j}\tilde{f}(t)$ is a linear combination of $f(t)$ and $\tilde{f}(t)$, which are mutually orthogonal. This representation is shown pictorially in Fig. 2(a).

Consider next the expansion of $f^a(t)$ over $f(t)$ and $\tilde{f}_\phi(t)$:

$$f^a(t)=\beta_1 f(t)+\beta_2\tilde{f}_\phi(t).$$

A function and its fractional Hilbert transform are, in general, not orthogonal. Hence, β_1 and β_2 cannot be directly obtained by considering projections of $f^a(t)$ onto $f(t)$ and $\tilde{f}_\phi(t)$. To compute β_1 and β_2, we use the following equality derived from (4):

$$\tilde{f}_\phi(t)=f(t)\cos\phi+\tilde{f}(t)\sin\phi. \tag{8}$$

Substituting (8) in $f^a(t)=f(t)+\mathrm{j}\tilde{f}(t)$ gives

$$\begin{aligned} f^a(t)&=f(t)+\mathrm{j}\frac{1}{\sin\phi}(\tilde{f}_\phi(t)-f(t)\cos\phi)\\ &=\left(1+\mathrm{j}\frac{\cos\phi}{\sin\phi}\right)f(t)+\left(\frac{\mathrm{j}}{\sin\phi}\right)\tilde{f}_\phi(t)=\beta_1 f(t)+\beta_2\tilde{f}_\phi(t), \end{aligned}$$

where $\beta_1=\operatorname{cosec}\phi e^{\mathrm{j}(\phi-\pi/2)}$ and $\beta_2=\operatorname{cosec}\phi e^{\mathrm{j}\pi/2}$. The construction of the $\phi-$AS is illustrated geometrically in Fig. 2(b). We observe that $f^a(t)$ can also be constructed from $f(t)$ and $\tilde{f}_\phi(t)$.

3. Properties of the $\phi-$analytic signal

3.1. Invariances

(I1) *Linearity*:
$\mathcal{A}_\phi\{\alpha_1 f_1+\alpha_2 f_2\}(t)=\alpha_1\mathcal{A}_\phi\{f_1\}(t)+\alpha_2\mathcal{A}_\phi\{f_2\}(t)$, for complex scalars α_1 and α_2.
(I2) *Shift-invariance*: $\mathcal{S}_\tau\mathcal{A}_\phi\{f\}(t)=\mathcal{A}_\phi\mathcal{S}_\tau\{f\}(t)$, for $\tau\in\mathbb{R}$.
(I3) *Scale-invariance*: $\mathcal{D}_\sigma\mathcal{A}_\phi\{f\}(t)=\mathcal{A}_\phi\mathcal{D}_\sigma\{f\}(t)$, for $\sigma\in\mathbb{R}^+$.

The proofs follow from the corresponding invariances of the fractional Hilbert operator $\mathcal{H}_\phi$, and from the definition of $\mathcal{A}_\phi$ given in (5).

3.2. Factorization

Let us analyze the action of the $\phi-$AS operator $\mathcal{A}_\phi$, on the product of two signals $f_1,f_2\in\mathbf{L}^2(\mathbb{R})$, where $\hat{f}_1(\omega)$ vanishes for $|\omega|\geq\omega_0$ and $\hat{f}_2(\omega)$ vanishes for $|\omega|<\omega_0$. It has been shown in [26] that, under these conditions, $\mathcal{H}_\phi$ satisfies the *generalized Bedrosian identity* [26,28]:

$$\mathcal{H}_\phi\{f_1 f_2\}(t)=f_1(t)\mathcal{H}_\phi\{f_2\}(t). \tag{9}$$

The generalized AS of $f_1(t)f_2(t)$ is given by

$$\begin{aligned} \mathcal{A}_\phi\{f_1 f_2\}(t)&=f_1(t)f_2(t)+e^{\mathrm{j}(\pi-\phi)}\mathcal{H}_\phi\{f_1 f_2\}(t)\\ &=f_1(t)(f_2(t)+e^{\mathrm{j}(\pi-\phi)}\mathcal{H}_\phi\{f_2\}(t))=f_1(t)\mathcal{A}_\phi\{f_2\}(t), \end{aligned} \tag{10}$$

where the second equality follows from (9). Thus, the $\phi-$AS of a product of two signals with disjoint spectra is equal to the product of the low-frequency signal and the $\phi-$AS of the high-frequency signal. We next consider an example illustrating this property.

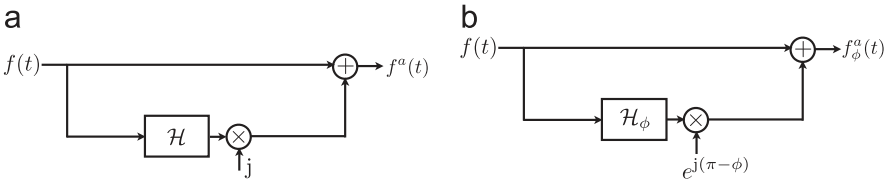

Fig. 1. Comparison of complex signal construction approaches: (a) Gabor's AS construction, and (b) $\phi-$AS construction using the FrHT.

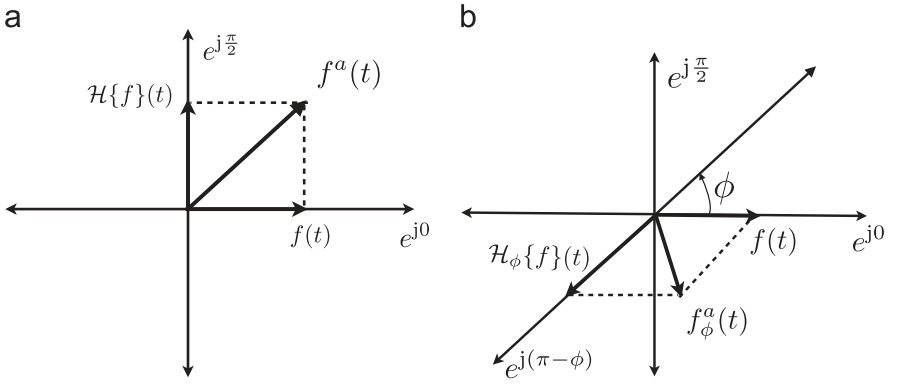

Fig. 2. Geometric vector interpretation of $\phi-$AS construction: (a) Gabor's AS construction ($\phi=\pi/2$), and (b) $\phi-$AS construction.

3.3. AM–FM representation

The AM and PM of an AM–FM signal $f(t)$ are defined as the modulus and phase angle of $f^a(t)$, respectively, and the FM is defined as the derivative of the PM [2]. Using (7), we write that

$$\left|f_\phi^a(t)\right| = |\sin\ \phi||f^a(t)| = |\sin\ \phi|a(t),$$

$$\theta_\phi(t) \triangleq \angle f_\phi^a(t) = \theta(t) + \frac{\pi}{2} - \phi + \pi\ \text{sign}(\sin\ \phi) \quad \text{and}$$

$$\omega_\phi(t) = \frac{\mathrm{d}}{\mathrm{d}t}\theta_\phi(t) = \omega(t). \tag{11}$$

We observe from (11) that the modulus of the ϕ−AS is equal to the AM scaled by a factor $|\sin\ \phi|$, its phase angle is equal to the PM offset by $\pi/2 - \phi + \pi\ \text{sign}(\sin\ \phi)$, and that the derivative of the phase angle is equal to the FM given by Gabor's AS.

3.4. Energy scaling

The energy of a real signal $f \in \mathbf{L}^2(\mathbb{R})$ is given by $E_f = \|f\|^2 = (1/2\pi)\|\hat{f}\|^2$ (Parseval's theorem). Let the energy of Gabor's AS $f^a(t)$ be denoted by E_f^a. Then, the energy of the ϕ−AS is given by

$$E_{f,\phi}^a = 2\ \sin^2\phi E_f^a, \tag{12}$$

which is a constant multiple of the signal energy. Gabor's AS corresponds to the case $\phi = \pi/2$, and hence $E_{f,\pi/2}^a = 2E_f^a$. For the case $\phi = \pi/4$, the energy of the ϕ−AS is given by $E_{f,\pi/4}^a = 2\ \sin^2(\pi/4)E_f^a = E_f^a$.

3.5. Temporal and spectral moments

We next compute the spectral moments using the ϕ−AS spectrum. We assume that, f in addition to being in $\mathbf{L}^2(\mathbb{R})$, also satisfies the following properties:

$$(1+|t|)^{n/2} f(t) \in \mathbf{L}^2(\mathbb{R}) \quad \text{and} \quad (1+|\omega|)^{n/2}\hat{f}(\omega) \in \mathbf{L}^2(\mathbb{R})$$

for $n \in \mathbb{N}$, so that the moments up to order n are well-defined. The n-th spectral moment of Gabor's AS is given by

$$\langle \omega^n \rangle = \frac{1}{E_f^a}\int_{-\infty}^{+\infty} \omega^n |\hat{f}^a(\omega)|^2\ \mathrm{d}\omega = \frac{2}{E_f}\int_0^{+\infty} \omega^n |\hat{f}(\omega)|^2\ \mathrm{d}\omega$$

and the n-th temporal moment is given by

$$\langle t^n \rangle = \frac{1}{E_f^a}\int_{-\infty}^{+\infty} t^n |f^a(t)|^2\ \mathrm{d}t.$$

Let $\langle t^n \rangle_\phi$ and $\langle \omega^n \rangle_\phi$ denote the n-th temporal and spectral moments of the ϕ−AS $f_\phi^a(t)$, respectively. Then, using (1), (6), and (12), we get that $\langle t^n \rangle_\phi = \langle t^n \rangle$ and $\langle \omega^n \rangle_\phi = \langle \omega^n \rangle$. The preceding analysis shows that Gabor's AS and the ϕ−AS have the same temporal and spectral moments. As a result, both analytic signals have the same time-bandwidth product and time–frequency localization property is not compromised on, in the process of generalization.

4. The generalized-phase Hilbert transform

We define the generalized-phase Hilbert transform of $f(t)$ in the frequency domain as

$$\hat{\tilde{f}}_g(\omega) = e^{-\mathrm{j}\phi(\omega)}\hat{f}(\omega)\mathcal{U}(\omega) + e^{\mathrm{j}\phi(\omega)}\hat{f}(\omega)\mathcal{U}(-\omega).$$

In the case when $\phi(\omega)$ is a scalar, the GPHT reduces to the FrHT. Let $\mathcal{H}_g$ denote the generalized-phase Hilbert operator such that $\tilde{f}_g(t) = \mathcal{H}_g\{f\}(t)$. We observe that the GPHT of $f(t)$ is expressible in the frequency domain as

$$\hat{\tilde{f}}_g(\omega) = \hat{h}_g(\omega)\hat{f}(\omega), \tag{13}$$

where $h_g(t) = \mathcal{F}^{-1}\{\hat{h}_g(\omega)\} = \mathcal{F}^{-1}\{e^{-\mathrm{j}\ \text{sign}(\omega)\phi(\omega)}\}$ denotes the convolutional kernel corresponding to the GPHT. Eq. (13) shows that the GPHT can be expressed as a linear filtering/convolution operation, that is,

$$\mathcal{H}_g\{f\}(t) = (h_g * f)(t), \tag{14}$$

which, in turn implies that $\mathcal{H}_g$ is a linear, shift-invariant operator. However, the GPHT convolutional kernel $h_g(t)$ is not always real-valued, unlike the FrHT kernel; depending on the nature of the phase kernel $\phi(\omega)$, the GPHT of a function may be real or complex. Let $\angle\hat{h}_g(\omega)$ denote the phase angle of $\hat{h}_g(\omega)$. Then, we get that

$$\angle\hat{h}_g(\omega) = \phi(\omega)\mathcal{U}(\omega) - \phi(\omega)\mathcal{U}(\omega) \quad \text{and}$$
$$\angle\hat{h}_g(-\omega) = \phi(-\omega)\mathcal{U}(-\omega) - \phi(-\omega)\mathcal{U}(-\omega). \tag{15}$$

In order that $h_g(t)$ be real, its FT should be conjugate-symmetric, that is, the phase angle of the FT, say $\theta(\omega)$, should be such that $\theta(-\omega) = -\theta(\omega)$ [29]. We observe from (15) that this is true when $\phi(\omega)$ is an even function of ω.

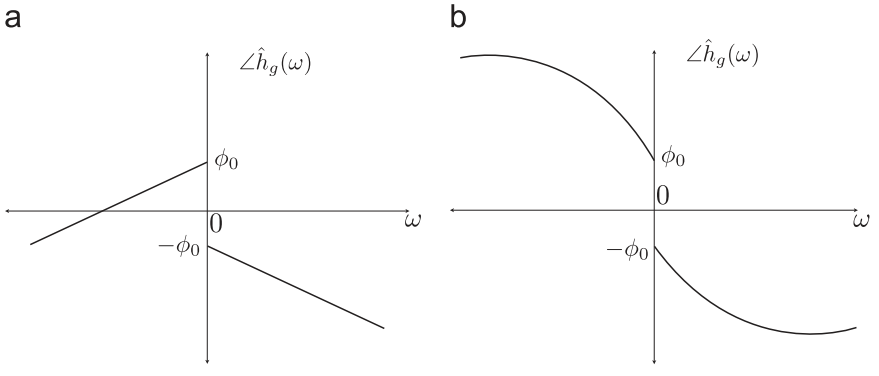

Fig. 3. Template of phase spectrum of GPHT kernel: (a) $\phi(\omega) = \phi_0 + \phi_1\omega$, and (b) $\phi(\omega) = \phi_0 + \phi_2\omega^2$.

Table 1
GPHT convolutional kernels corresponding to polynomial-phase kernels.

$\phi(\omega)$	$\tilde{h}_g(t)$
ϕ_0	$\cos\ \phi_0\delta(t) + \sin\ \phi_0\frac{1}{\pi t}$
$\phi_0+\phi_1\omega$	$\frac{\mathrm{j}}{2\pi(\phi_1^2-t^2)}e^{-\mathrm{j}\phi_0}(\phi_1(e^{2\mathrm{j}\phi_0}+1)+(e^{2\mathrm{j}\phi_0}-1)t)$
$\phi_0+\phi_2\omega^2$	$\frac{1}{4\sqrt{\pi\phi_2^3}}e^{-\mathrm{j}(4\phi_0\phi_2+t^2)/4\phi_2}\left(\sqrt{\phi_2}(\sqrt{\mathrm{j}\phi_2}e^{2\mathrm{j}\phi_0}+\sqrt{-\mathrm{j}\phi_2}e^{\mathrm{j}t^2/2\phi_2})\right.$ $\left.+(-1)^{1/4}\left\lvert\phi_2\right\rvert\left(\mathrm{j}e^{\mathrm{j}t^2/2\phi_2}\mathrm{Cerf}\left(\frac{(-1)^{1/4}t}{2\sqrt{\phi_2}}\right)+e^{2\mathrm{j}\phi_0}\mathrm{Cerf}\left(\frac{(-1)^{3/4}t}{2\sqrt{\phi_2}}\right)\right)\right)$

In the particular case when $\phi(\omega)$ is a polynomial, this requires that $\phi(\omega)$ be a function consisting only of even powers of ω. In Fig. 3(a) and (b), we show templates of the phase spectrum for two different GPHT kernels.

In Table 1, we list $h_g(t)$ for different types of polynomial-phase kernels. We observe that $h_g(t)$ is non-causal in all the cases. Although the functional form of $h_g(t)$ corresponding to $\phi(\omega)=\phi_0+\phi_1\omega^2$ contains complex-valued terms, it can be shown that $h_g(t)$ is indeed a real-valued function by using properties of the complex error function $\mathrm{Cerf}(\cdot)$ [30]. In Fig. 4(a)–(d), we show examples of impulse responses of linear-phase kernel and quadratic phase-kernel GPHTs. We observe that in the case when $\phi(\omega)=\phi_1\omega$, the GPHT convolutional kernel $h_g(t)=\phi_1/\pi(\phi_1^2-t^2)$ has singularities at $t=\phi_1$ and $t=-\phi_1$, and it decays as $1/t^2$, unlike the FrHT kernel (including the standard HT), which has a singularity at $t=0$ and decays only as $1/t$. This, in turn implies that the GPHT of a function, evaluated using $\phi(\omega)=\phi_1\omega$, exhibits better decay properties than the corresponding FrHT. In the case when $\phi(\omega)=\phi_2\omega^2$, however, $h_g(t)$ is an oscillating function, and does not decay with time. In Table 2, we show $h_g(t)$ computed for $\phi(\omega)=0.3\omega$, and $\phi(\omega)=0.4\omega^2$ and the corresponding phase spectra. It can be shown that the GPHT convolutional kernel diverges as $|t|$ tends to infinity for polynomial-phase kernels of orders larger than 2, and therefore, we shall not consider them in further analysis. The adjoint of the operator $\mathcal{H}_g$, which we shall denote by $\mathcal{H}_g^\dagger$, is expressible as the following convolution operation $\langle t^n\rangle_\phi=\langle t^n\rangle$ and $\langle\omega^n\rangle_\phi=\langle\omega^n\rangle$, where $h_g^{-1}(t)\triangleq\mathcal{F}^{-1}\{[\hat{h}_g(\omega)]^*\}=\mathcal{F}^{-1}\{e^{\mathrm{j}\ \mathrm{sign}(\omega)\phi(\omega)}\}$, which follows from the observation that $\hat{h}_g(\omega)(\hat{h}_g(\omega))^*=1$.

4.1. Properties of the GPHT

(Q1) $\mathcal{H}_g$ maps $\mathbf{L}^2(\mathbb{R})$ functions to $\mathbf{L}^2(\mathbb{R})$.
(Q2) *Linearity*:
$\mathcal{H}_g\{\alpha_1f_1+\alpha_2f_2\}(t)=\alpha_1\mathcal{H}_g\{f_1\}(t)+\alpha_2\mathcal{H}_g\{f_2\}(t)$, for α_1 and α_2 in the complex field $\mathbb{C}$.
(Q3) *Shift-invariance*: $\mathcal{S}_\tau\mathcal{H}_g\{f\}(t)=\mathcal{H}_g\mathcal{S}_\tau\{f\}(t)$, for $\tau\in\mathbb{R}$.
(Q4) *Scale-invariance*: $\mathcal{D}_\sigma\mathcal{H}_g\{f\}(t)=\mathcal{H}_g\mathcal{D}_\sigma\{f\}(t)$, for $\sigma\in\mathbb{R}^+$.
(Q5) *Orthogonality*: If $f_1,f_2\in\mathbf{L}^2(\mathbb{R})$ such that $\langle f_1,f_2\rangle=0$, then $\langle\tilde{f}_{1g},\tilde{f}_{2g}\rangle=0$.
(Q6) *Linear independence*: If $\{f_i(t)\}_{i=1}^N$ constitutes a set of linearly independent functions, so does $\{\mathcal{H}_g\{f_i\}(t)\}_{i=1}^N$.

Property (Q1) can be proved using the convolution property of the FT and the identity: $\hat{h}_g(\omega)(\hat{h}_g(\omega))^*=1$. Properties (Q2), (Q3), and (Q4) follow from the observation that the GPHT is associated with a convolutional kernel. The property (Q5) can be proved by proceeding along the same lines as in the proof of property (P4) of the FrHT in Section 2.3.

Proof of (Q6). Let $\{f_i(t)\}_{i=1}^N$ denote a set of N linearly independent functions, that is, $\sum_{i=1}^N\alpha_if_i(t)=0,\forall t\Rightarrow\alpha_i=0,\forall i$. Consider the linear combination:

$$\sum_{i=1}^N\beta_i\tilde{f}_{i,g}(t)=\sum_{i=1}^N\beta_i\mathcal{H}_g\{f_i\}(t)=\sum_{i=1}^N\mathcal{H}_g\{\beta_if_i(t)\}$$
$$=\mathcal{H}_g\left\{\sum_{i=1}^N\beta_if_i(t)\right\},\tag{16}$$

where the last equality follows from the linearity of $\mathcal{H}_g$. If $f_i(t)\neq0,\forall i$, the linear combination in (16) equals zero only if $\mathcal{H}_g\{\sum_{i=1}^N\beta_if_i(t)\}=0,\forall t$, which implies $\beta_i=0\forall i$. This implies that, similar to the FrHT case, the GPHT can be used to generate new bases from an existing linearly independent bases.

4.2. Selective enhancement of singularities

Davis et al. [15] showed that the FrHT can be used for enhancement and selective highlighting of falling/rising edges; the selectivity in highlighting one edge over the other depends on the magnitude and polarity of the FrHT phase parameter ϕ. We show that a similar property holds for the GPHT for particular forms of $\phi(\omega)$. Consider the symmetric rectangular pulse $f(t)=\mathbf{1}_{[-3,3]}$. We compute the GPHT of $f(t)$ corresponding to the phase kernel $\phi(\omega)=\phi_0+\phi_1\omega$. We consider two different cases: (i) $|\phi_0|=0.1$, $|\phi_1|=0.1$, and (ii) $|\phi_0|=0.5$, $|\phi_1|=0.1$, that is, four different combinations of (ϕ_0,ϕ_1) for each case. In Fig. 5(a)–(e), we show the magnitude of the GPHT of $1_{[-3,3]}$ for different cases. We observe that in both cases, different edges are selected depending on the polarities of ϕ_0 and ϕ_1. In the first case, the falling edge is highlighted when both ϕ_0 and ϕ_1 have the same polarities, and the rising edge is highlighted when they have opposite polarities. In the second case, however, the rising edge is highlighted when the polarity of $\phi_0<0$ and the falling edge is highlighted in case of $\phi_0>0$, irrespective of the polarity of ϕ_1. This shows that the edge highlighting behavior depends on the relative magnitudes of ϕ_0 and ϕ_1. For the case when $\phi(\omega)=\phi_2\omega^2$, $h_g(t)$ is an oscillating non-decaying function and is unsuitable for edge highlighting/enhancement.

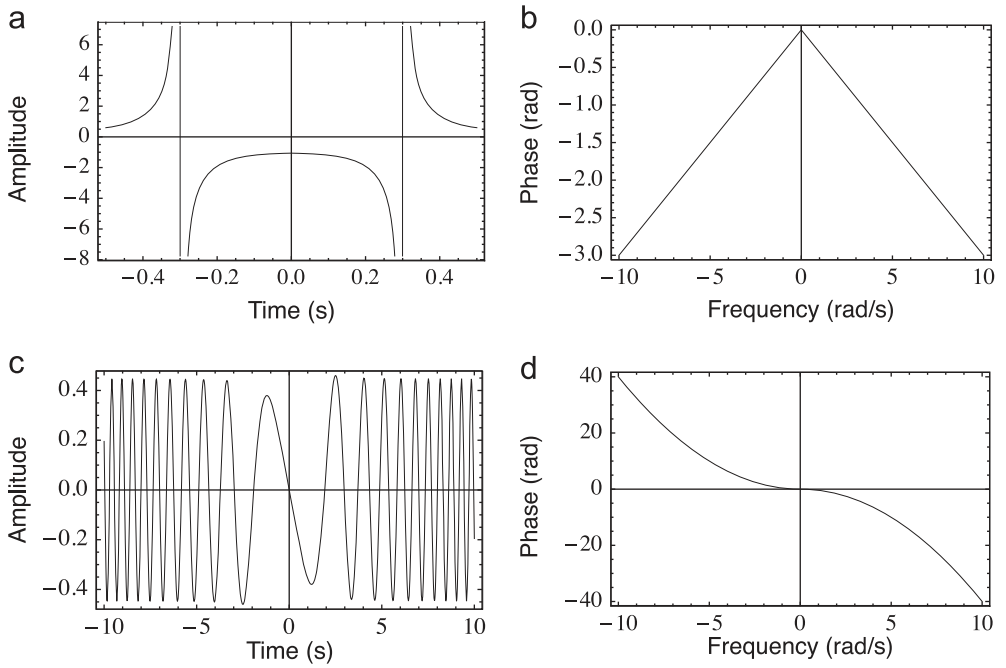

Fig. 4. GPHT impulse responses and phase spectra. (a) The imaginary part of $h_g(t)$ for $\phi(\omega)=0.3\omega$ (the real part is zero) and (b) the corresponding phase response; (c) the real part of $h_g(t)$ for $\phi(\omega)=0.4\omega^2$ (the imaginary part is zero) and (d) the corresponding phase response.

Table 2
GPHT convolutional kernels computed for particular values of ϕ_0, ϕ_1, and ϕ_2.

$\phi(\omega)$	$\tilde{h}_g(t)$
0.1	$0.995\delta(t)+0.09\frac{1}{\pi t}$
0.3ω	$\frac{9.5493\mathrm{j}}{100t^2-0.9}$
$0.4\omega^2$	$\mathrm{Real}\{(-0.157-\mathrm{j}0.157)e^{-\mathrm{j}0.625t^2}\,\mathrm{Cerf}((0.559-\mathrm{j}0.559)t)\}$

4.3. GPHT and Lie group connection

Chaudhury and Unser showed that FrHTs form a commutative group [26,33]. In a technical note [34], Chaudhury also gave a Lie group characterization of the notions of steerability [35] (which is useful for directional image analysis) and shiftability (which is an important aspect in complex wavelet design [26]). We next review Lie groups briefly and show that GPHTs also constitute a Lie group.

A group G is said be a Lie group if the composition operation $G\times G$ and the inversion operation G^{-1} are continuous [36]. In particular, consider the group parameterized by a scalar parameter ϕ, that is, $G=(G_\phi)_\phi$ for ϕ lying on some smooth manifold, such as $\mathbb{R}$. Then, G is said to be a Lie group if the composition and inversion maps, represented as $(\phi_1,\phi_2)\to\mathrm{Comp}(\phi_1,\phi_2)$ and $\phi\to\mathrm{Inv}(\phi)$, respectively, are infinitely differentiable over their respective parameters, that is, $\mathrm{Comp}(\phi_1,\phi_2)$ and $\mathrm{Inv}(\phi)$ are smooth functions of (ϕ_1,ϕ_2) and ϕ, respectively.

Consider the group of GPHTs corresponding to monomial phase functions, that is, $\phi(\omega)=\phi\omega^i$. The GPHT of $f(t)$ has the FT $e^{-\mathrm{j}\phi\omega^i\,\mathrm{sign}(\omega)}\hat{f}(\omega)$. Let $\mathcal{H}_{g_1}$ and $\mathcal{H}_{g_2}$ denote the GPHT operators corresponding to $\phi_1(\omega)=\phi_1\omega^i$ and $\phi_2(\omega)=\phi_2\omega^i$, respectively. Then, the FT of the composition $\mathcal{H}_{g_1}\mathcal{H}_{g_2}\{f\}(t)$ is given by $e^{-\mathrm{j}(\phi_1+\phi_2)\omega^i\,\mathrm{sign}(\omega)}\hat{f}(\omega)$, which shows that the composition of $\mathcal{H}_{g_1}$ and $\mathcal{H}_{g_2}$ is equal to the GPHT corresponding to $\phi(\omega)=(\phi_1+\phi_2)\omega^i$, that is, $\mathrm{Comp}(\phi_1,\phi_2)=\phi_1+\phi_2$. The operator $\mathcal{H}_g^\dagger$, which is the inverse of $\mathcal{H}_g$, corresponds to GPHT with $\phi(\omega)=(-\phi)\omega^i$, that is, $\mathrm{Inv}(\phi)=-\phi$. Thus, both composition and inversion maps are infinitely differentiable, and hence, the GPHTs corresponding to monomial phase functions form a Lie group, which is a superset of the Lie group of FrHTs.

The generator $\mathcal{G}$ of a Lie group (G_ϕ) is defined as [36]

$$\mathcal{G}\{f\}\triangleq\frac{\mathrm{d}}{\mathrm{d}\phi}G_\phi\{f\}\Big|_{\phi=0},\quad \phi\in\mathbb{R},$$

where the domain of $\mathcal{G}$ is the space of square-integrable functions. Then, the Lie group (G_ϕ) can be characterized using $\mathcal{G}$ as follows:

$$G_\phi f=e^{\phi\mathcal{G}}f\quad\text{where } e^{\phi\mathcal{G}}=\mathcal{I}+\phi\mathcal{G}+\frac{1}{2!}\phi^2\mathcal{G}^2+\cdots.$$

The generator of the Lie group constituted by GPHTs has the following frequency-domain manifestation:

$$\mathcal{G}\{\hat{f}\}(\omega)=\frac{\mathrm{d}}{\mathrm{d}\phi}\mathcal{H}_g\{\hat{f}\}(\omega)\Big|_{\phi=0}=\frac{\mathrm{d}}{\mathrm{d}\phi}(e^{-\mathrm{j}\phi\omega^i\,\mathrm{sign}(\omega)}\hat{f}(\omega))\Big|_{\phi=0}$$

$$=-\mathrm{j}\omega^i\,\mathrm{sign}(\omega)\hat{f}(\omega)=\omega^i\hat{\tilde{f}}(\omega).$$

Using the differentiation property of the Fourier transform, we get that $\mathcal{G}$ has the following time-domain

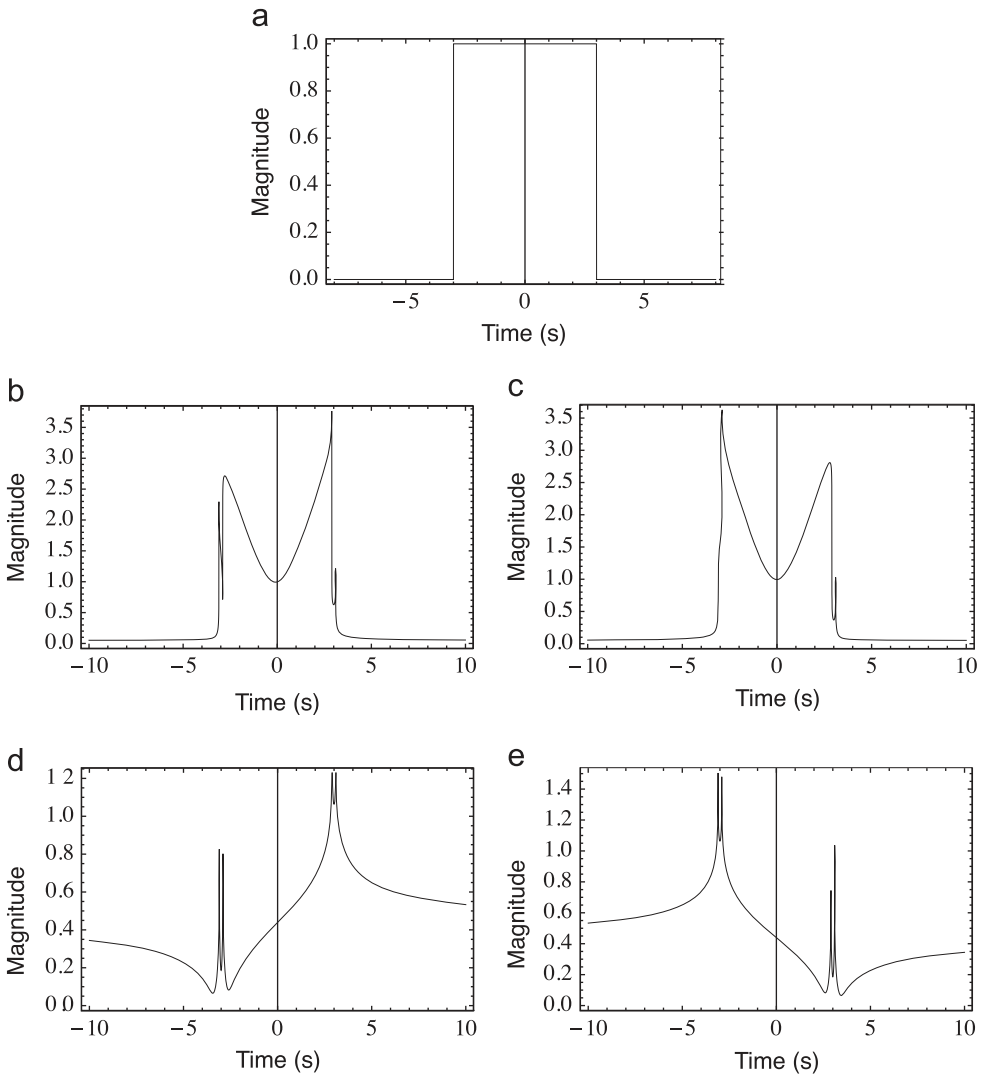

Fig. 5. Edge-enhancement and selectivity of the GPHT: (a) $\mathbf{1}_{[-3,3]}$, (b) $\phi(\omega)=0.1+0.1\omega$ (or $\phi(\omega)=-0.1-0.1\omega$), (c) $\phi(\omega)=-0.1+0.1\omega$ (or $\phi(\omega)=0.1-0.1\omega$), (d) $\phi(\omega)=0.5+0.1\omega$ (or $\phi(\omega)=0.5-0.1\omega$), and (e) $\phi(\omega)=-0.5+0.1\omega$ (or $\phi(\omega)=-0.5-0.1\omega$).

description:

$$\mathcal{G}\{f\}(t)=(-\mathrm{j})^i\frac{\mathrm{d}^i}{\mathrm{d}t^i}\mathcal{H}\{f\}(t).$$

The exponentiation of $\mathcal{G}$ is given by

$$e^{\phi\mathcal{G}}\{\hat{f}\}(\omega)=e^{\mathrm{j}\phi\omega^i\ \mathrm{sign}(\omega)}\hat{f}(\omega)=\mathcal{F}\{\mathcal{H}_g\{f\}\}(\omega)=\mathcal{H}_g\{\mathcal{F}\{f\}\}(\omega),$$

which shows that the group of GPHTs is obtained by exponentiation of the generator $\mathcal{G}$. Though we have considered only monomial phase functions, the analysis may be suitably extended to other polynomial phase functions.

5. The generalized-phase analytic signal

We next construct a function $\hat{f}_g^a(\omega)$ in the frequency domain as follows:

$$\hat{f}_g^a(\omega)=\hat{f}(\omega)+e^{\mathrm{j}(\pi-\phi(\omega))}\hat{\tilde{f}}_g(\omega). \tag{17}$$

Following similar analysis as in (6), we simplify (17) to

$$\hat{f}_g^a(\omega)=\sin\ \phi(\omega)e^{\mathrm{j}(\pi/2-\phi(\omega))}\hat{f}^a(\omega), \tag{18}$$

which vanishes for $\omega<0$. Thus, $f_g^a(t)$ represents a further extension of the $\phi-$AS construction, which we shall refer to as the *generalized-phase AS* (*GPAS*). The function $\phi(\omega)$ should be chosen such that $\sin\ \phi(\omega)$ does not vanish over a finite-length interval; otherwise, the spectral information is lost and recovery of $f(t)$ from $f_g^a(t)$ is impossible. Taking the inverse FT on both sides of (17) gives

$$f_g^a(t)=f(t)+\mathcal{F}^{-1}\{e^{\mathrm{j}(\pi-\phi(\omega))}\hat{\tilde{f}}_g(\omega)\}. \tag{19}$$

Since $(f_1{*}f_2)(t)\overset{\mathcal{F}}{\longleftrightarrow}\hat{f}_1(\omega)\hat{f}_2(\omega)$, we rewrite (19) equivalently as

$$f_g^a(t)=f(t)+\ell(t){*}\tilde{f}_g(t), \tag{20}$$

where $\ell(t)=\mathcal{F}^{-1}\{e^{\mathrm{j}(\pi-\phi(\omega))}\}$, which must be interpreted in the distributional sense. Let $\mathcal{L}$ denote the convolutional

operator associated with the kernel $\ell(t)$, that is, $\mathcal{L}\{f\}(t) = (\ell * f)(t)$. Then, we get that

$$f_g^a(t) = f(t) + \mathcal{L}\mathcal{H}_g\{f\}(t). \tag{21}$$

In Fig. 6, we show the construction of the GPAS using the GPHT. Eq. (18) can be rewritten as

$$\hat{f}_g^a(\omega) = \hat{\alpha}(\omega)\hat{f}^a(\omega), \tag{22}$$

where $\hat{\alpha}(\omega) = \sin\phi(\omega)e^{j(\pi/2-\phi(\omega))}$. Taking the inverse FT on both sides of (22), we get that $f_g^a(t) = (\alpha * f^a)(t)$, that is, the GPAS is obtained from Gabor's AS through a linear filtering operation, such that the filter has the impulse response $\alpha(t) = \mathcal{F}^{-1}\{\sin\phi(\omega)e^{j(\pi/2-\phi(\omega))}\}$. This also implies that $f^a(t)$ can be obtained from $f_g^a(t)$ through the inverse filter whose impulse response is given by $\alpha^{-1}(t) = \mathcal{F}^{-1}\{\operatorname{cosec}\ \phi(\omega)e^{j(\phi(\omega)-\pi/2)}\}$ such that $f_g^a(t) = (\alpha^{-1} * f_g^a)(t)$. In Table 3, we give the expressions for $\alpha(t)$ and $\alpha^{-1}(t)$ corresponding to different polynomial-phase kernels. Since $f(t) = \text{Real}\{f^a(t)\}$, we get from (18) that

$$f(t) = \text{Real}\{\mathcal{F}^{-1}\{\operatorname{cosec}\phi(\omega)e^{-j(\phi(\omega)-\pi/2)}\hat{f}_g^a(\omega)\}\}. \tag{23}$$

We note from (21), that the GPAS also satisfies properties of linearity, shift-invariance, and scale-invariance, similar to the ϕ−AS. We next consider specific examples of linear and quadratic phase functions.

5.1. Linear phase function: $\phi(\omega) = \phi_0 + \phi_1\omega$

In this case, $\ell(t) = e^{j(\pi-\phi_0)}\delta(t+\phi_1)$, and substituting $\ell(t)$ into (20), we get that

$$f_g^a(t) = f(t) + e^{j(\pi-\phi_0)}\delta(t+\phi_1) * \mathcal{H}_g\{f\}(t). \tag{24}$$

The corresponding FT is given by

$$\hat{f}_g^a(\omega) = 2\ \sin(\phi_0 + \phi_1\omega)e^{j(\pi/2-(\phi_0+\phi_1\omega))}\hat{f}(\omega)\mathcal{U}(\omega).$$

5.2. Quadratic phase function: $\phi(\omega) = \phi_0 + \phi_1\omega + \phi_2\omega^2$

A quadratic-phase kernel in frequency is associated with a quadratic-phase function in time as shown by the Fourier pair: $\sqrt{(j/4\pi\phi_2)}e^{j(t+\phi_1)^2/4\phi_2} \overset{\mathcal{F}}{\longleftrightarrow} e^{j(\phi_1\omega+\phi_2\omega^2)}$. Then, we get that

$$\ell(t) = \mathcal{F}^{-1}\{e^{j(\pi-(\phi_0+\phi_1\omega+\phi_2\omega^2))}\} = -\sqrt{\frac{j}{4\pi\phi_2}}e^{j((t+\phi_1)^2/4\phi_2-\phi_0)}. \tag{25}$$

Substituting (25) in (20) gives

$$f_g^a(t) = f(t) - \left(\sqrt{\frac{j}{4\pi\phi_2}}e^{j((t+\phi_1)^2/4\phi_2-\phi_0)} * \mathcal{H}_g\{f\}(t)\right). \tag{26}$$

The corresponding FT is given by

$$\hat{f}_g^a(\omega) = 2\ \sin(\phi_0 + \phi_1\omega + \phi_2\omega^2)\ e^{j(\pi/2-(\phi_0+\phi_1\omega+\phi_2\omega^2))}\hat{f}(\omega)\mathcal{U}(\omega). \tag{27}$$

By setting $\phi_0 = \phi_1 = 0$ in (26), we get that

$$\tilde{f}_g(t) = \mathcal{F}^{-1}\{e^{-j\phi_2\omega^2}\hat{f}(\omega)\mathcal{U}(\omega) + e^{j\phi_2\omega^2}\hat{f}(\omega)\mathcal{U}(-\omega)\} \quad \text{and}$$

$$f_g^a(t) = f(t) - \left(\sqrt{\frac{j}{4\pi\phi_2}}e^{jt^2/4\phi_2} * \mathcal{H}_g\{f\}(t)\right). \tag{28}$$

The quadratic-phase GPHT, the generalized HT (GHT) proposed by Zayed [17], and the generalized analytic signal proposed by Fu and Li [22] involve the use of quadratic chirps, but the chirping takes place in different domains and in different ways. We shall explain this aspect further. The GHT is constructed by multiplying the signal with a quadratic chirp in time, followed by convolution with the standard Hilbert convolutional kernel, and dechirping in time-domain, whereas the GPHT is obtained by multiplying the signal spectrum with frequency-domain chirps: the positive and negative frequencies are multiplied with chirps of opposite slopes. The GAS of Fu and Li is based on a two-parameter (a,b) Hilbert transform, which reduces to the Hilbert transform used by Zayed if the two-parameter version is constrained by considering $a/2b$ to be the parameter. Fu and Li further apply the LCT to make the signal analytic in the LCT domain.

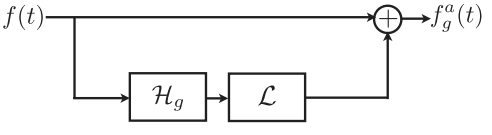

Fig. 6. Construction of the ϕ−AS using the generalized-phase HT.

Table 3
$\alpha(t)$ and $\alpha^{-1}(t)$ for certain phase kernels.

$\phi(\omega)$	$\alpha(t)$	$\alpha^{-1}(t)$
ϕ_0	$\sin\phi_0 e^{j(\pi/2-\phi_0)}\delta(t)$	$\operatorname{cosec}\phi_0 e^{j(\phi_0-\pi/2)}\delta(t)$
$\phi_1\omega$	$0.5\delta(t)-0.5\delta(t+2\phi_1)$	$\frac{-j}{2\phi_1}\cot(\frac{\pi t}{2\phi_1})$
$\phi_2\omega^2$	$\frac{j\sqrt{j\phi_2}}{4\phi_2\sqrt{2\pi}}e^{jt^2/8\phi_2}+\frac{1}{2}\delta(t)$	Intractable

6. Causality and the ϕ−analytic signal

A signal $f(t)$ is said to be causal if it vanishes for $t<0$. The real and imaginary parts of the FT of a causal signal form a HT pair, that is, $\hat{f}(\omega) = \hat{f}_R(\omega) + j\hat{f}_I(\omega)$, where $\hat{f}_R(\omega)$ and $\hat{f}_I(\omega)$ denote the real and imaginary parts of the $\hat{f}(\omega)$, respectively, such that $\hat{f}_I(\omega) = \mathcal{H}\{\hat{f}_R(\omega)\}$ [29,31,32]. Clearly, a causal signal and Gabor's AS are time–frequency duals and therefore, the ϕ−AS construction proposed in Section 2 can be extended to causal signals as well. In particular, consider the following spectral representation:

$$\hat{f}_c(\omega) = \hat{f}_R(\omega) + e^{j(\pi-\phi)}\mathcal{H}_\phi\{\hat{f}_R\}(\omega) = \mathcal{A}_\phi\{\hat{f}_R\}(\omega),$$

where the operator $\mathcal{A}_\phi$ acts in the frequency domain. We observe that $\hat{f}_c(\omega)$ is the ϕ−AS of the real function $\hat{f}_R(\omega)$ in the frequency domain, such that the corresponding time function is causal. Using (7), we get that $\hat{f}_c(\omega) = \sin\phi e^{j(\pi/2-\phi)}\mathcal{A}\{\hat{f}_R\}(\omega)$, and since $\mathcal{A}\{\hat{f}_R\}(\omega) = \hat{f}(\omega)$, we get that

$$\hat{f}_c(\omega) = \sin\phi e^{j(\pi/2-\phi)}\hat{f}(\omega) \quad \text{or}$$

$$f(t) = \operatorname{cosec}\phi e^{j(\phi-\pi/2)}f_c(t) = \mathcal{F}^{-1}\{\mathcal{A}_\phi\{\hat{f}_R(\omega)\}\}.$$

This implies that it is possible to characterize a family of causal functions using the FrHT: a real frequency function combined with its standard HT in quadrature results in a causal signal, whereas appropriate linear combination of the frequency function with its FrHT also results in a causal signal. Proceeding along similar lines, it can be shown that causal signals can also be characterized using the GPHT proposed in Section 4, that is, the signal constructed in the frequency domain as

$$\hat{f}_{c,g}(\omega) = \hat{f}_R(\omega) + \mathcal{L}\mathcal{H}_g\{\hat{f}_R\}(\omega), \tag{29}$$

is causal. We considered the characterization of causal signals using $\hat{f}_R(\omega)$ and its FrHT/GPHT. Analogously, we can characterize causal signals using $\hat{f}_I(\omega)$ and its FrHT/GPHT.

Consider the causal signal $f(t) = \mathbf{1}_{[\tau_1-\tau/2,\tau_1+\tau/2]}$, which is the indicator function for the interval $[\tau_1-\tau/2, \tau_1+\tau/2]$, such that $\tau_1 > \tau/2$. Its FT is given by $\hat{f}(\omega) = \tau\,\mathrm{sinc}(\omega\tau/2)e^{-\mathrm{j}\omega\tau_1}$. Correspondingly, the real part $\hat{f}_R(\omega) = \tau\,\mathrm{sinc}(\omega\tau/2)\cos(\omega\tau_1)$. The FrHT of $\hat{f}_R(\omega)$ is given by $\mathcal{H}_\phi\{\hat{f}_R\}(\omega) = \tau\,\mathrm{sinc}(\omega\tau/2)\cos(\omega\tau_1-\phi)$, where we have used the generalized Bedrosian identity [26]; the condition $\tau_1 > \tau/2$ ensures that the signal obeys the separability condition required for the theorem to be applicable. In Fig. 7(a) and (b), we show $\hat{f}_R, \hat{f}_I$, and $\mathcal{H}_\phi\{\hat{f}_R\}$ corresponding to the case when $\tau = 2$ and $\tau_1 = 3$, and the FrHT phase $\phi = -3\pi/4$. From (29), we get that

$$\begin{aligned}\hat{f}_c(\omega) &= \tau\,\mathrm{sinc}\left(\frac{\omega\tau}{2}\right)\cos(\omega\tau_1) - e^{\mathrm{j}\phi}\tau\,\mathrm{sinc}\left(\frac{\omega\tau}{2}\right)\cos(\omega\tau_1-\phi)\\ &= \tau\,\mathrm{sinc}\left(\frac{\omega\tau}{2}\right)\left(\cos(\omega\tau_1) - e^{\mathrm{j}\phi}\cos(\omega\tau_1-\phi)\right)\\ &= \sin\phi\, e^{\mathrm{j}(\omega\tau+\phi-\pi/2)}\tau\,\mathrm{sinc}\left(\frac{\omega\tau}{2}\right).\end{aligned} \tag{30}$$

Taking the inverse FT on both sides of (30), we get that

$$\begin{aligned}f_c(t) &= \sin\phi\, e^{\mathrm{j}(\pi/2-\phi)}\mathcal{F}^{-1}\left\{\tau\,\mathrm{sinc}\left(\frac{\omega\tau}{2}\right)e^{-\mathrm{j}\omega\tau_1}\right\}\\ &= \sin\phi\, e^{\mathrm{j}(\pi/2-\phi)}f(t),\end{aligned}$$

that is, $f_c(t)$ is a scaled version of the causal function $f(t)$, and is causal as well. This implies that the causal $f(t)$ is expressible using $\hat{f}_R(\omega)$ and its FrHT, just as the $\hat{f}_R(\omega)$ and its standard HT is used to describe $f(t)$.

7. Application to secure single-sideband modulation scheme

The AS is employed in communication systems through the single-sideband modulation (SSB) scheme, which results in bandwidth savings by a factor of two compared to the baseband signal. For the purposes of security, a secret key is often employed such that perfect recovery of the signal is possible only with the knowledge of the key [18,21]. We show next that it is possible to develop a secure SSB system with multiple secret keys using the GPHT proposed in Section 4, which includes the FrHT as a special case.

Consider the case of GPHT with polynomial-phase kernel, that is, $\phi(\omega) = \sum_{i=0}^{2}\phi_i\omega^i$, using which we construct the GPAS $f_g^a(t)$. As noted in Section 4, phase kernels of orders larger than two lead to diverging GPHT convolutional kernels, such that the inverse GPHT is ill-posed. Hence, we shall consider only the second-order polynomial case. From (23), we observe that, in order to construct $f(t)$ from $f_g^a(t)$, we need prior knowledge of the key vector $[\phi_0, \phi_1, \phi_2]$. Motivated by this observation, we propose a secure SSB scheme that uses $[\phi_0, \phi_1, \phi_2]$ as the secret key vector. As shown in Fig. 8(a)–(d), the signal $f(t)$ is encoded using the phase kernel $\phi(\omega)$, to generate the GPAS $f_g^a(t)$, which is transmitted after modulating with a carrier of frequency ω_c. At the receiver, $y(t)$ is demodulated to get $f_g^a(t)$, which is further decoded using the phase kernel $\phi(\omega) + \Delta\phi$. Unless the phase kernel/key vector used at receiver end coincides exactly with that used for encoding (that is, $\Delta\phi = 0$), the decoded signal will differ from the desired message $f(t)$, and the decoded signal will only be an approximation of $f(t)$, which we denote by $\bar{f}(t)$. Errors are also introduced due to the presence of noise in the channel. In what follows, we first analyze sensitivity of the decoding process with respect to key perturbation $\Delta\phi$, assuming noise-free conditions, followed by performance analysis in the presence of additive channel noise, for three specific cases of $\phi(\omega)$, and we use the frequency-domain implementation of the operators for this purpose.

7.1. Effect of key perturbations

We consider the effect of key perturbations $\Delta\phi$ on the received signal, assuming noiseless transmission. By following the block diagrams in Fig. 8(c) and (d), we get that

$$\bar{f}(t) = \mathrm{Real}\left\{\mathcal{F}^{-1}\left\{\frac{\sin\phi(\omega)}{\sin(\phi(\omega)+\Delta\phi)}e^{-\mathrm{j}(\Delta\phi)}\hat{f}^a(\omega)\right\}\right\}. \tag{31}$$

We consider three specific cases of the phase kernel, namely, $\phi(\omega) = \phi_0$, $\phi(\omega) = \phi_1\omega$, and $\phi(\omega) = \phi_2\omega^2$. The corresponding perturbations are given by $\Delta\phi = \Delta\phi_0$, $\Delta\phi = \Delta\phi_1\omega$, and $\Delta\phi = \Delta\phi_2\omega^2$, respectively. In Fig. 9(a)–(c), we show the energy of the error $E_{(f-\bar{f})}$ as a function of $\Delta\phi_i/\phi_i \times 100$, for $i = 0, 1, 2$, expressed as a percentage of the signal energy

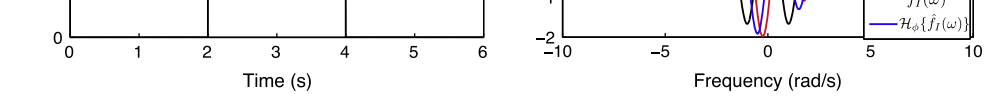

Fig. 7. Characterization of causal signals using the FrHT: (a) signal $f(t) = \mathbf{1}_{[2,3]}$ and (b) spectral functions. The black and red curves indicate the real and imaginary parts of $\hat{f}(\omega)$, respectively. The blue curve depicts $\mathcal{H}_\phi\{\hat{f}_R\}(\omega)$ for $\phi = -3\pi/4$. (For interpretation of the references to color in this figure caption, the reader is referred to the web version of this article.)

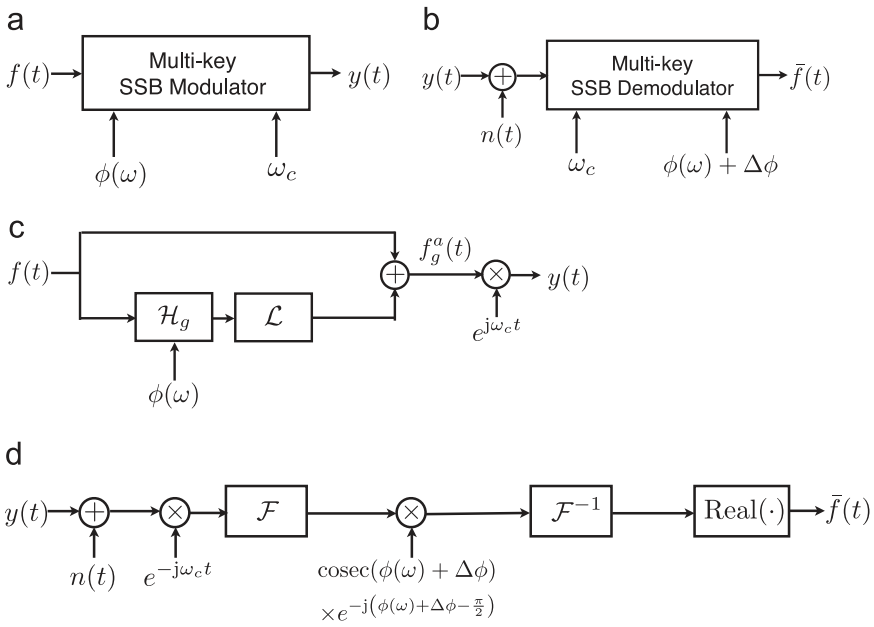

Fig. 8. Multi-key secure SSB modulation scheme: (a) modulator, (b) demodulator, (c) details of the modulator, and (c) details of the demodulator.

E_f, corresponding to the AM–FM signal $f(t)=(1+0.5\cos(10\pi t))\cos(50\pi t)$, for the interval $[0,1]$ seconds, after multiplying with a Hamming window. In each case, the analysis is carried out for key values lying in the interval $[-\pi,+\pi]$ in steps of 0.1π. We observe that the error plots are asymmetric with respect to the perturbation: the error is larger for negative perturbations. As expected, the error is zero for all the three cases when the perturbation is zero. In each case, the error plots corresponding to negative key values coincide with those obtained for positive key values. In the cases $\phi(\omega)=\phi_1\omega$ and $\phi(\omega)=\phi_2\omega^2$, for a given $\Delta\phi$, the plots for different encode key values almost coincide, unlike the $\phi(\omega)=\phi_0$ case, where different encode key values lead to different error plots. Also, for a given perturbation, larger the magnitude of the encode key, larger the error. This characteristic can be explained with the help of (31). Assuming that $\Delta\phi$ is sufficiently small, we get that $\sin(\phi(\omega)+\Delta\phi)\approx\sin\ \phi(\omega)$ and $e^{-j\Delta\phi}\approx 1-j\Delta\phi$, (31) can be simplified as

$$\bar{f}(t)=\mathrm{Real}\{\mathcal{F}^{-1}\{1-j\Delta\phi_i\omega^i\}\hat{f}^a(\omega)\}$$
$$=f(t)-\phi_i\mathrm{Real}\left\{\mathcal{F}^{-1}\left\{j\left(\frac{\Delta\phi_i}{\phi_i}\right)\omega^i\hat{f}^a(\omega)\right\}\right\},$$

that is, for a given fractional perturbation $\Delta\phi_i/\phi_i$, the error $f(t)-\bar{f}(t)$ is directly proportional to the key value ϕ_i, and the magnitude of the error is not affected by the polarity of ϕ_i. Consequently, the SSB scheme allows for security in the form of the phase kernel keys, a feature not possessed by Gabor's AS-based SSB.

7.2. Effect of noise

We next consider the performance of the proposed secure SSB scheme under noisy conditions. We use the test signal $f(t)$ and the GPHT phase kernels considered in Section 7.1. We assume that the encode and decode keys coincide, so that no errors are introduced due to key perturbations. The channel noise is modeled as additive, complex, white Gaussian noise such that the real and imaginary components of the noise add to the real and imaginary parts of the GPAS, respectively. The experiment is performed at different signal-to-noise ratio (SNR) levels. For a particular GPHT kernel, the MSE values are obtained by averaging over 2000 repeated trials of the experiment. From Fig. 10(a)–(c), we observe that the MSE decreases as the SNR increases. We notice that in the case when $\phi(\omega)=\phi_0$, the noise performance for different key values coincide. In the case when $\phi(\omega)=\phi_1\omega$, for a given SNR, the MSE increases as $|\phi_1|$ increases, as shown in Fig. 10(b). We also observe similar behavior in the case when $\phi(\omega)=\phi_2\omega^2$ as shown in Fig. 10(c). Since the MSE increases with the magnitude of ϕ_1 and ϕ_2, it is preferable to use keys of moderate magnitudes in the communication process. Although we have considered the design of a secure SSB system using polynomial-phase kernels, in principle, more sophisticated phase functions could be employed. For example, the linear phase kernel may be generalized to a piecewise-linear function, thereby introducing more security keys.

We next compare the performance of the proposed secure SSB with that of the secure SSB proposed by Tao et al. [21] (which we shall refer to as SSB-Tao). Tao et al. used the following FrFT-based FrHT definition:

$$h_{\alpha,\varphi}(t)=\cos\ \varphi e^{-j(t^2/2)\cot\alpha}f(t)+\sin\ \varphi e^{-j(t^2/2)\cot\alpha}\tilde{f}(t), \qquad (32)$$

and the corresponding analytic signal is obtained as

$$s_{\alpha,\varphi}(t)=e^{-j(t^2/2)\cot\alpha}f(t)-e^{-j\varphi}h_{\alpha,\varphi}(t).$$

SSB-Tao employs two secret keys, α and φ. In the particular case when $\cot\alpha=0$, $h_{\alpha,\varphi}(t)=\cos\ \varphi f(t)+\sin\ \varphi\tilde{f}(t)=\tilde{f}_\varphi(t)$, and hence, SSB-Tao coincides with the proposed secure

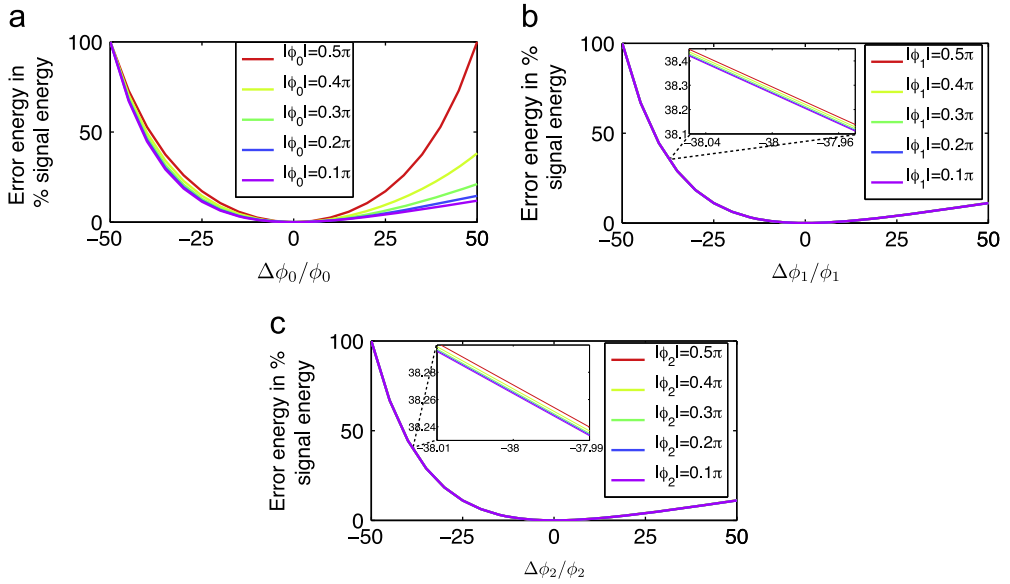

Fig. 9. Error energy versus key perturbation for different values of security key ϕ_2: (a) $\phi(\omega)=\phi_0$, (b) $\phi(\omega)=\phi_1\omega$, and (c) $\phi(\omega)=\phi_2\omega^2$.

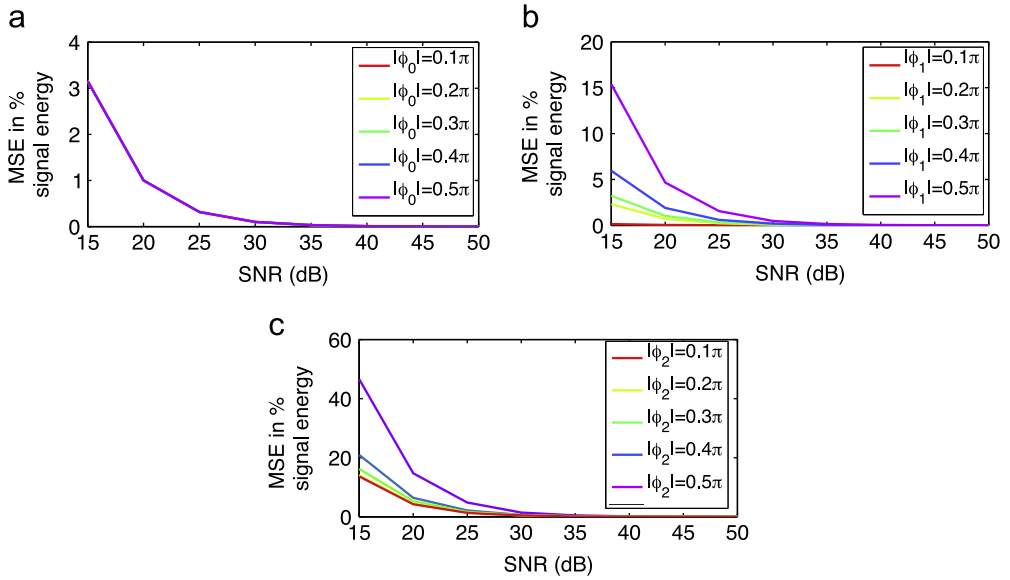

Fig. 10. MSE as a function of SNR, expressed in percentage signal energy: (a) $\phi(\omega)=\phi_0$, (b) $\phi(\omega)=\phi_1\omega$, and (c) $\phi(\omega)=\phi_2\omega^2$.

SSB scheme (which we shall refer to as SSB-GPHT), corresponding to $\phi(\omega)=\varphi$. In the case when $\cot\alpha\neq 0$, we compare the performance of SSB-Tao with that of SSB-GPHT with two secret keys, that is, when $\phi(\omega)=\phi_0+\phi_1\omega$. The values of ϕ_0 and ϕ_1 are chosen to be equal to 0.1π and 0.1π, respectively, according to MSE plots in Fig. 10(a) and (b), to result in good noise performance. Since the role of φ in $h_{\alpha,\varphi}(t)$ is equivalent to that of ϕ_0 in GPHT, we choose $\varphi=\phi_0=0.1\pi$ and vary α over $[0.1\pi, 0.9\pi]$. We consider performance of SSB-Tao and SSB-GPHT when applied to the signal $f(t)=(1+0.5\sin(10t))\cos(500t+0.01\sin(30t))$. In Fig. 11(a), we show the MSE variation of SSB-Tao scheme as a function of SNR and α. We observe that, for a given SNR, the MSE does not vary significantly with α. In Fig. 11 (b), we show the MSE versus SNR plots for the two methods when $\alpha=0.5\pi$. We observe that for a given SNR, the MSE of the SSB-Tao is larger than that of SSB-GPHT. Though our formalism is in the continuous-time domain, we have used the corresponding discrete-time implementation for experimental validation, in which case, the ϕ−AS coincides with that proposed by Tseng et al. [18].

8. Conclusion

We proposed a generic construction of the AS based on the FrHT. This signal is referred to as the ϕ−AS and is dependent on the phase of the fractional Hilbert operator.

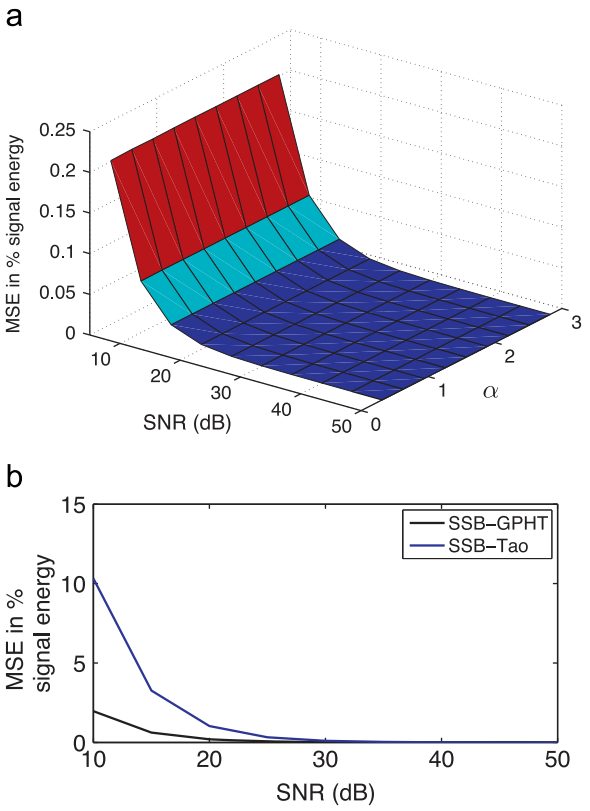

Fig. 11. (a) Noise performance of SSB-Tao and (b) comparison of noise performance of SSB-Tao and SSB-GPHT.

The classical Gabor's construction becomes a special case of our construction. We also gave a geometric interpretation of the new method, which gives rise to the ϕ–AS naturally. The ϕ–AS enjoys important invariances and factorization properties similar to Gabor's AS. It also satisfies the same time–frequency localization properties (Heisenberg's uncertainty principle). This approach led us to a further generalization, where the fractional Hilbert operator is replaced by a phase function leading to the GPHT. We showed that the GPHT possesses many of the properties of the FrHT, including selective enhancement and highlighting of edges, and a connection with Lie groups. We also proposed the generalized-phase AS, which is a generalization of the ϕ–AS using the GPHT, and showed that the GPAS and Gabor's AS are related by a linear filtering operation. We showed that it is possible to characterize causal signals in terms of the FrHT/GPHT, by identifying the duality between the notions of analyticity and causality. As an application of the GPAS, we developed a multi-key secure SSB modulation scheme. Decode key perturbation analysis and noise-performance analysis showed that the proposed SSB scheme has the potential for incorporating additional security into communication systems.

The proposed GPHT may also be employed to transform orthonormal bases and since the transformation is unitary, certain smoothness and decay properties may be preserved, although localization properties may not be preserved. A recent seminal contribution in this direction was made by Chaudhury and Unser [37], who addressed the question in the general setting of non-compactly supported wavelet bases and showed that the Hilbert transform of a wavelet is again a wavelet and that the transformation preserves smoothness and decay properties. With regard to localization, Chaudhury and Unser showed that it is controlled by the number of vanishing moments of the original wavelet. Since the GPHTs are a functional generalization of the standard HT, it would be possible to perform a characterization of the GPHTs of wavelets in terms of the associated smoothness, decay, and localization, along the lines of [37].

Acknowledgments

The authors would like to acknowledge the support received from the Indian Space Research Organization – Indian Institute of Science Space Technology Cell.

References

[1] D. Gabor, Theory of communication, Journal of Institute of Electrical Engineers 93 (1946) 429–457.
[2] L. Cohen, Time–Frequency Analysis: Theory and Applications, Prentice-Hall, Inc., Upper Saddle River, NJ, USA, 1995.
[3] L. Cohen, P. Loughlin, D. Vakman, On an ambiguity in the definition of the amplitude and phase of a signal, Signal Processing 79 (1999) 301–307.
[4] S.L. Hahn, On the uniqueness of the definition of the amplitude and phase of the analytic signal, Signal Processing 83 (2003) 1815–1820.
[5] L. Cohen, P. Loughlin, Authors' reply, Signal Processing 83 (2003) 1821–1822.
[6] B. Picinbono, On instantaneous amplitude and phase of signals, IEEE Transactions on Signal Processing 45 (1997) 552–560.
[7] R. Kumaresan, A. Rao, Model-based approach to envelope and positive instantaneous frequency estimation of signals with speech applications, Journal of the Acoustical Society of America 105 (1999) 1912–1924.
[8] M.I. Doroslovački, On nontrivial analytic signals with positive instantaneous frequency, Signal Processing 83 (2003) 655–658.
[9] P. Dang, T. Qian, Analytic phase derivatives, all-pass filters and signals of minimum phase, IEEE Transactions on Signal Processing 59 (2011) 4708–4718.
[10] X.-G. Xia, L. Cohen, On analytic signals with nonnegative instantaneous frequencies, in: IEEE International Conference on Acoustics, Speech, and Signal Processing, vol. 3, 1999, pp. 1329–1332.
[11] G.-T. Deng, T. Qian, An application of entire function theory to analytic signals, Journal of Mathematical Analysis and Applications 389 (2012) 54–57.
[12] A.W. Lohmann, D. Mendlovic, Z. Zalevsky, Fractional Hilbert transform, Optics Letters 21 (1996) 281–283.
[13] H. Ozaktas, D. Mendlovic, Fourier transforms of fractional order and their optical interpretation, Optics Communications 101 (1993) 163–169.
[14] E. Sejdić, I. Djurović, L. Stanković, Fractional Fourier transform as a signal processing tool: An overview of recent developments, Signal Processing 91 (2011) 1351–1369.
[15] J.A. Davis, D.E. McNamara, D.M. Cottrell, Analysis of the fractional Hilbert transform, Applied Optics 37 (1998) 6911–6913.
[16] S.C. Pei, M.H. Yeh, Discrete fractional Hilbert transform, IEEE Transactions on Circuits and Systems II: Analog and Digital Signal Processing 47 (2000) 1307–1311.
[17] A.I. Zayed, Hilbert transform associated with the fractional Fourier transform, IEEE Signal Processing Letters 5 (1998) 206–208.
[18] C.C. Tseng, S.C. Pei, Design and application of discrete-time fractional Hilbert transformer, IEEE Transactions on Circuits and Systems II: Analog and Digital Signal Processing 47 (2000) 1529–1533.
[19] S.C. Pei, P.H. Wang, Analytical design of maximally flat FIR fractional Hilbert transformers, Signal Processing 81 (2001) 643–4661.
[20] A. Cusmariu, Fractional analytic signals, Signal Processing 82 (2002) 267–272.

[21] R. Tao, X.M. Li, Y. Wang, Generalization of the fractional Hilbert transform, IEEE Signal Processing Letters 15 (2008) 365–368.
[22] Y. Fu, L. Li, Generalized analytic signal associated with linear canonical transform, Optics Communications 281 (2008) 1468–1472.
[23] X. Guanlei, W. Xiaotong, X. Xiaogang, Generalized Hilbert transform and its properties in 2D LCT domain, Signal Processing 89 (2009) 1395–1402.
[24] S. Sarkar, K. Mukherjee, A. Ray, Generalization of Hilbert transform for symbolic analysis of noisy signals, Signal Processing 89 (2009) 1245–1251.
[25] J. Ge, C. Wang, X. Zhu, Fractional optical Hilbert transform using phase shifted fiber Bragg gratings, Optics Communications 284 (2011) 3251–3257.
[26] K.N. Chaudhury, M. Unser, On the shiftability of dual-tree complex wavelet transforms, IEEE Transactions on Signal Processing 58 (2010) 221–232.
[27] K.N. Chaudhury, M. Unser, Construction of Hilbert transform pairs of wavelet bases and Gabor-like transforms, IEEE Transactions on Signal Processing 57 (2009) 3411–3424.
[28] E. Bedrosian, A product theorem for Hilbert transforms, Proceedings of IEEE 51 (1963) 868–869.
[29] R. Bracewell, The Fourier Transform and its Applications, third ed. McGraw-Hill, New York, 1999.
[30] M. Abramowitz, I.A. Stegun, Error function and Fresnel integrals, in: Handbook of Mathematical Functions with Formulas, Graphs, and Mathematical Tables, 9th ed., Dover, NY, 1972, pp. 297–309 (Chapter 7).
[31] A.V. Oppenheim, R.W. Schafer, J.R. Buck, Discrete-Time Signal Processing, second ed. Prentice-Hall, Inc., Upper Saddle River, NJ, 1999.
[32] J.S. Toll, Causality and the dispersion relation: Logical foundations, Physical Review 104 (1956) 1760–1770.
[33] K.N. Chaudhury, Optimally Localized Wavelets and Smoothing Kernels, Swiss Federal Institute of Technology Lausanne, EPFL, Thesis no. 4968, February 16, 2011.
[34] K.N. Chaudhury, Lie Group Characterization of Steerability and Shiftability, Technical Note. URL: ⟨http://bigwww.epfl.ch/chaudhury/liegroups.pdf⟩.
[35] W.T. Freeman, E.H. Adelson, The design and use of steerable filters, IEEE Transactions on Pattern Analysis and Machine Intelligence 13 (1991) 891–906.
[36] P.C. Teo, Y. Hel-Or, Canonical decomposition of steerable functions, Journal of Mathematical Imaging and Vision 13 (1998) 83–95.
[37] K.N. Chaudhury, M. Unser, On the Hilbert transform of wavelets, IEEE Transactions on Signal Processing 59 (2011) 1890–1894.